

**ULTRASOUND DOPPLER FLOW MEASUREMENTS
IN A LIQUID METAL COLUMN
UNDER THE INFLUENCE OF A STRONG
AXIAL ELECTRIC CURRENT**

*M. Starace, N. Weber, M. Seilmayer, C. Kasprzyk,
T. Weier, F. Stefani, S. Eckert*

*Institute of Fluid Dynamics, Helmholtz-Zentrum Dresden–Rossendorf, Bautzner
Landstraße 400, 01328 Dresden, Germany*

Magnetohydrodynamic instabilities can constitute a serious hazard to the functionality of liquid metal batteries. Here we consider the Tayler instability, which appears when the electric current, passing through a conducting fluid, reaches a critical value. The experiment discussed in this article involves a column of a eutectic GaInSn alloy, along whose axis an electric current passes. Ultrasound transducers encased in a copper electrode bounding the top of the column were used to obtain the vertical component of fluid flow, once a noise suppression system had been devised. The data thus retrieved will be discussed here.

Introduction. Because the amount of fossil and nuclear fuels available on the Earth is limited and because some of the effects resulting from their extraction and use may compromise the habitability of our planet, or parts thereof, societies are investing more heavily in the electricity generation from renewable sources, such as wind and solar energy. As the amount of energy produced by such means is intrinsically dependent on uncontrollable meteorological factors of limited predictability, it is necessary to store excess energy in order for it to be available when the demand in it surpasses the supply. Liquid metal batteries (LMBs) have been proposed as a practicable technology to compensate for rapidly fluctuating differences in energy production and consumption on a large scale. Small scale prototypes have shown that some of their advantages are a long cycle life, a high current density ($\approx 10 \text{ kA/m}^2$), good scalability, low cost of the cathode, anode and electrolyte materials, as well as their self-assembling stratification and simplicity of the batteries' construction [1, 2]. These advantages are contrasted by low output voltages ($\lesssim 1 \text{ V}$) as well as by elevated working temperatures necessary for the metal electrodes and molten salt electrolytes to remain liquid. Moreover, MHD instabilities caused by the charging and discharging processes are likely to occur in LMBs larger than the prototypes tested so far. Such instabilities could cause a local displacement of the electrolyte layer and bring the electrodes in direct contact, which would short out the battery.

It is not useful to prevent short circuits due to the mixing of the liquid electrode phases by simply making the electrolyte layer sufficiently thick, as this would increase its internal resistance and reduce the maximum current achievable by the cells. However, other means of suppressing such instabilities have already been proposed, such as returning the current from one electrode through a borehole in the battery out of the other extremity of the battery [3], or leading the current around the battery through axial or horizontal Helmholtz coils [4]. The first of these would reshape the destabilizing radial magnetic field distribution, whereas the other two would generate stabilizing axial and horizontal fields, respectively.

As liquid GaInSn is incompressible, the instability under consideration here is the kink type Tayler instability (TI), which is the counterpart of the kink mode ($m = 1$) instability of the z -pinch in compressible plasma [5]. The instability is driven by a current I_z passing vertically (hence, the z -pinch) through the GaInSn cylinder, much as it would in an LMB. This results in an azimuthal magnetic field B_ϕ , which in turn causes a radial Lorentz force F_r^L pointing inward. If the radial dependence of the magnetic field behaves as

$$\frac{\partial \left(r B_\phi^2(r) \right)}{\partial r} > 0 \quad (1)$$

in a perfectly conducting and inviscid medium of homogeneous density, such a scenario would exhibit a non-axisymmetric instability [6]. Slight perturbations of the fluid would result in a breaking of cylindrical symmetry of the \mathbf{B} -field, bunching the field lines on one side and spreading them on the other, which in turn would break the cylindrical symmetry of \mathbf{F}^L and cause the perturbations to grow exponentially. In a fluid with finite viscosity, electrical resistivity and density stratification such perturbations would be damped at low magnetic flux densities. However, if they surpass some critical value, the TI [7] manifests itself as a column of vortices with a specific periodicity (Fig. 1). Assuming an initially uniform current distribution, this criterion is met at Hartmann numbers $\text{Ha} = BR\sqrt{\sigma/\rho\nu} \approx 21$ in our setup, where R is the GaInSn cylinder's radius, σ is the electrical conductivity, ρ is the mass density and ν its kinematic viscosity [8, 9].

Previous measurements performed with fluxgate magnetometers determined the minimum current required to drive the kink mode instability to be ≈ 2.7 kA [10],

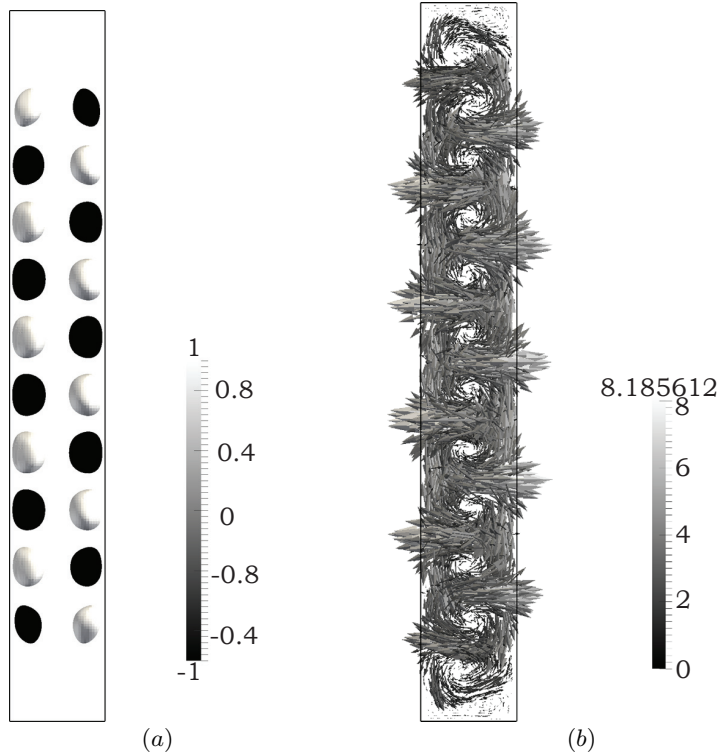


Fig. 1. Simulated saturated TI at a current of 10 kA [9]. (a) B_z contours, [μT]; (b) velocity field v , [mm/s].

whereas the sausage, or varicose mode ($m = 0$) instability was predicted not to occur at finite currents. The experiment has since been modified in such a way that the vertical component of GaInSn flow within the column can be measured directly with ultrasound Doppler velocimetry (UDV).

1. Experimental setup.

1.1. Basic setup. The experimental setup consists of a 75 cm long polyoxymethylene (POM) tube, whose internal diameter is 10 cm, which is filled with a eutectic GaInSn alloy. Copper electrodes, connected to a switching mode DC power supply unit (PSU) via 3 cm wide hollow copper leads, are attached to the cylinder's top and bottom. The bottom electrode, the PSU and the hollow connectors are water-cooled. In order to facilitate a stable density stratification, the top electrode is left uncooled.

The Power Station pe5030-W PSU, which was manufactured by plating electronic GmbH, has a switching frequency of 10 kHz. It can attain a maximum voltage of 6 V and a maximum current of 8 kA. To facilitate UDV, two cylindrical holes were drilled into the top electrode, parallel to the column's axis, into which ultrasound transducers (USTs) were inserted to directly couple with the liquid metal (Fig. 2). The USTs have a diameter of 12 mm, are optimized to operate at 6 MHz and can safely sustain temperatures of up to 60 °C. Their piezoelectric crystals are triggered by a Doppler velocimeter, which also records the echoes reflected off the bottom electrode and scattering particles within the liquid and is controlled by a data acquisition computer. The vertical position and velocity components of the scatterers are computed by the velocimeter in real time from the echoes' delays and frequency shifts. These tracer particles are not deliberately introduced, but

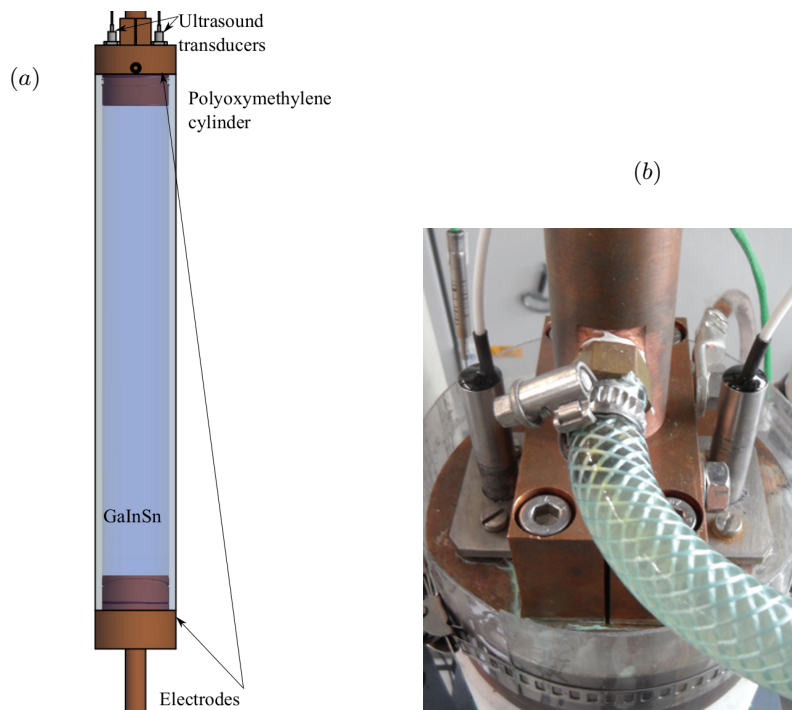


Fig. 2. The Tayler experiment. (a) Schematic of the GaInSn cylinder. (b) Top electrode with USTs.

consist of solid metal oxides, as well as of GaInSn particles solidified by localized deviations from the eutectic mixture.

Although transducers optimized for lower frequencies would have been sufficient for the spatial and temporal scales of interest here, it was discovered that low frequency transducers recorded significantly more noise when currents of the order of 1 kA were passing through the system. The most likely reason for the higher frequency USTs' lower susceptibility to noise is the fact that the PSU operates at a switching frequency of 10 kHz and that its rectangular waveform can be represented as a superposition of sinusoidal waves of odd integer multiples of 10 kHz and exponentially decreasing amplitude.

1.2. Noise damping system. Despite the use of higher frequency transducers, the amount of noise at high currents was still too large for any velocimetry data to be obtained at all [11]. The power supply circuit was, therefore, upgraded with a noise reduction system consisting of six film capacitors and 14 VITROPERM[®] (a nanocrystalline FeCuNbSiB alloy), carbonyl iron and hydrogen-reduced iron powder ring cores.

The capacitors, which were manufactured by Electronicon Kondensatoren GmbH, are connected to the PSU's mains in parallel to the TI experiment and to each other, acting as a shunt damping DC ripple currents. Their self-inductance is 15 nH with capacitances and equivalent series resistances ranging from 0.47 to 50 μ F and 0.2 to 2.9 m Ω , respectively.

The ring cores were placed around the copper feeding leads conducting the current to and from the Tayler experiment. The set consists of five carbonyl iron cores of type T225-2, which were manufactured by Amidon Inc. and six VITROPERM[®] ones of type T60004-L2160-W631 (abbreviated as W631 from now on), manufactured by Sekels GmbH. The cores induce a voltage in the direction opposite to any change in current, thus damping AC ripples. They have high inductive reactances in the frequency range used for UDV. The relative permeability of the two core types is $\mu_r = 10$ and $\mu_r = 17250$, respectively. The saturation flux density for iron powder materials, below which the magnetic flux density increases linearly with the magnetic field strength, is 1 T. Within this linear regime, the inductance is constant. Using Ampère's circuital law, it can be estimated that the T225-2 cores are not saturated even at the 1.5 cm radius of the copper leads and 8 kA, the maximum current achievable by the PSU used here. Due to no better alternatives being available at the time of their purchase (spring 2012), the W631 cores do reach saturation. Moreover, two ring cores of type W631, as well as one type T650-36 hydrogen-reduced iron core with $\mu_r = 75$, were used as a common-mode choke (CMC). Despite the high relative permeability of these cores, they should not reach saturation flux density, as DC currents through the two conductors they surround flow in opposite directions, causing their associated magnetic fields to nearly cancel each other out (Fig. 3).

The coaxial cables connecting the USTs to the Doppler velocimeter were coiled around the ring and split ferrite cores to reduce sheath currents running along the cables. Furthermore, ground loops with other nearby electrical equipment would have caused the velocimeter to be at a floating common potential. To stabilize the potential, the velocimeter had to be separated galvanically by connecting it to an isolation transformer. In addition to this, the top electrode encasing the USTs was grounded.

2. Results. The simulated result for the critical current at which the TI sets in is approximately 2.7 kA with a periodicity of its vortices along the z -axis of $\lambda \approx 12.5$ cm, or $\lambda^{-1} \approx 8$ m⁻¹, as was verified by Seilmayer *et al.* through

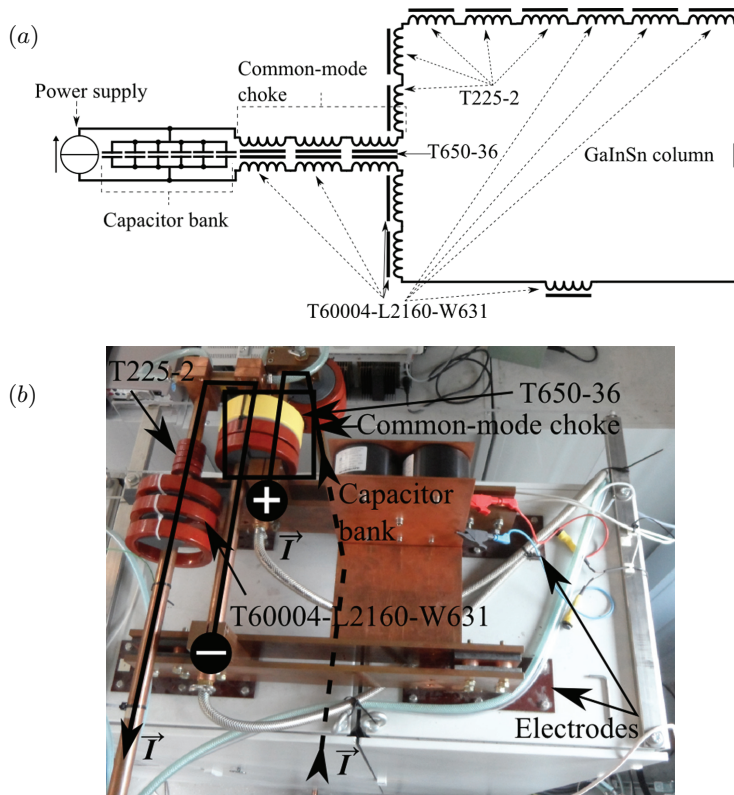


Fig. 3. Noise suppression system. (a) Circuit diagram of the experiment's main components. (b) Noise suppression assembly on top of the PSU.

B_z measurements [9, 10]. However, other processes, chiefly thermal convection caused by ohmic losses and electro-vortex flow induced by the non-uniform current distribution at the interfaces between the electrodes and the GaInSn column, set in at lower currents. The latter is further exacerbated by the holes in the top electrode accommodating the ultrasound sensors. Moreover, the axial asymmetry of the \mathbf{B} -field inherent in the experimental setup due to the single turn coil consisting of the the GaInSn column and the copper leads connecting it to the PSU is likely to have an effect as well.

The vertical components of the tracer particles' velocities in the GaInSn column were retrieved at currents ranging from 2.00 to 4.00 kA in steps of 0.25 kA. Depending on the current, measurement times could not exceed 25 to 45 minutes, as the uncooled top electrode's temperature would otherwise have surpassed 50 °C, the maximum temperature at which the POM cylinder can be safely operated. Figs. 4a and 4b display the vertical velocity profiles of the tracer particles in the GaInSn column measured by the two USTs. The current was switched on at $t = 0$ and brought to a supercritical value of 3.75 kA in approximately 30 seconds. Each transducer measured upward and downward motion which alternated spatially, both along the depth of the cylinder and between the two transducers. This would seem to suggest the presence of vortices expected for the TI, as seen in Fig 1.

In order to better understand the observed flow patterns and any spatial periodicity within them, spectral analyses of the velocity profiles were carried out. Figs. 4c and 4d show a least squares spectral density estimation (SD) in arbitrary

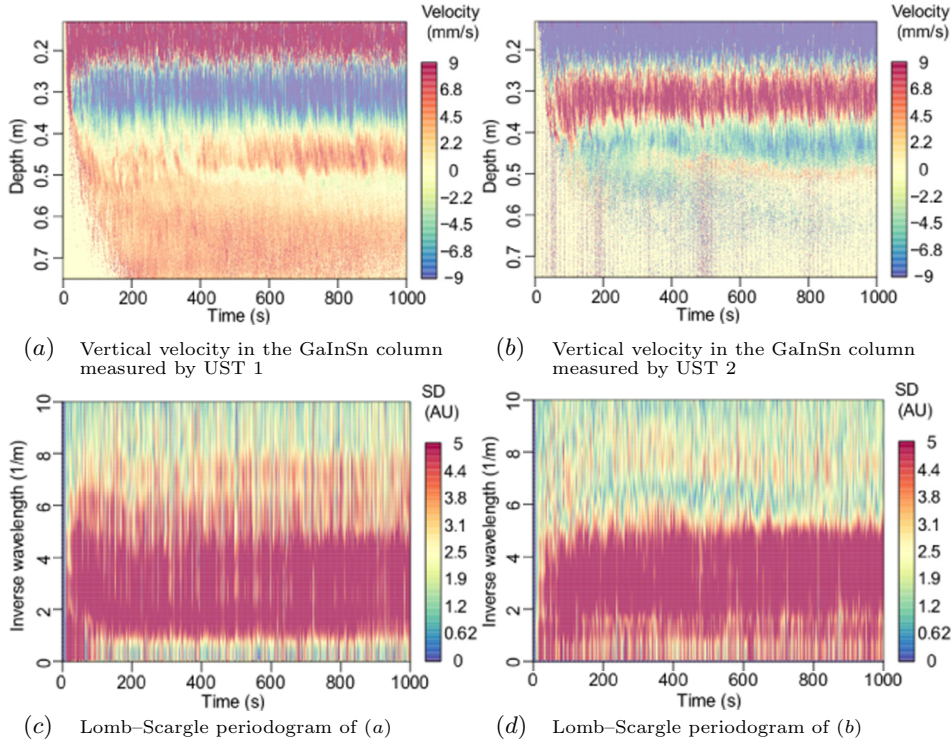


Fig. 4. Velocity profiles and periodograms at 3.75 kA.

units (AU) using the Lomb-Scargle method [12] for the velocimetry data from Figs. 4a and 4b, respectively.

There is a mode close to the expected periodicity of 8 m^{-1} , yet it is eclipsed by a much more predominant mode of approximately half that inverse wavelength. The presence of this mode was also found by the B_z measurements of Seilmayer *et al.* [10]. Although the cause of this deviation from the expected characteristic λ^{-1} is not fully understood, it can now be ruled out that aliasing artefacts of the slightly under-resolved fluxgate magnetometer measurements are to blame.

Velocity profiles and their corresponding periodograms for a sub-critical current of 2.00 kA are shown in Fig. 5. The current is increased from 0 to 2.00 kA in the first 30 seconds and maintained for 840 seconds. Both the profile and the spectral density exhibit similar patterns to those at supercritical currents, indicating further that phenomena other than the TI may be responsible for some of the fluid's movement, even at supercritical currents. However, the 8 m^{-1} mode is not present in this subcritical measurement. The disappearance of the flow pattern as soon as the current is switched off 870 s into the measurement may hint that it is mostly a current-driven rather than a thermal convective phenomenon.

It is noteworthy that in Figs. 4a, 4b, 5a and 5b the fluid initiates its vertical motion close to the top electrode at first, while the content of the bottom part of the cylinder only starts moving vertically after approximately three minutes. This hints at a motion driven by the non-uniform current density at the top electrode. Two-dimensional simulations investigating the relation between the electro-vortex flow and the non-uniformity of current distribution at the interface between the top electrode and the liquid metal at the interaction with thermal convection

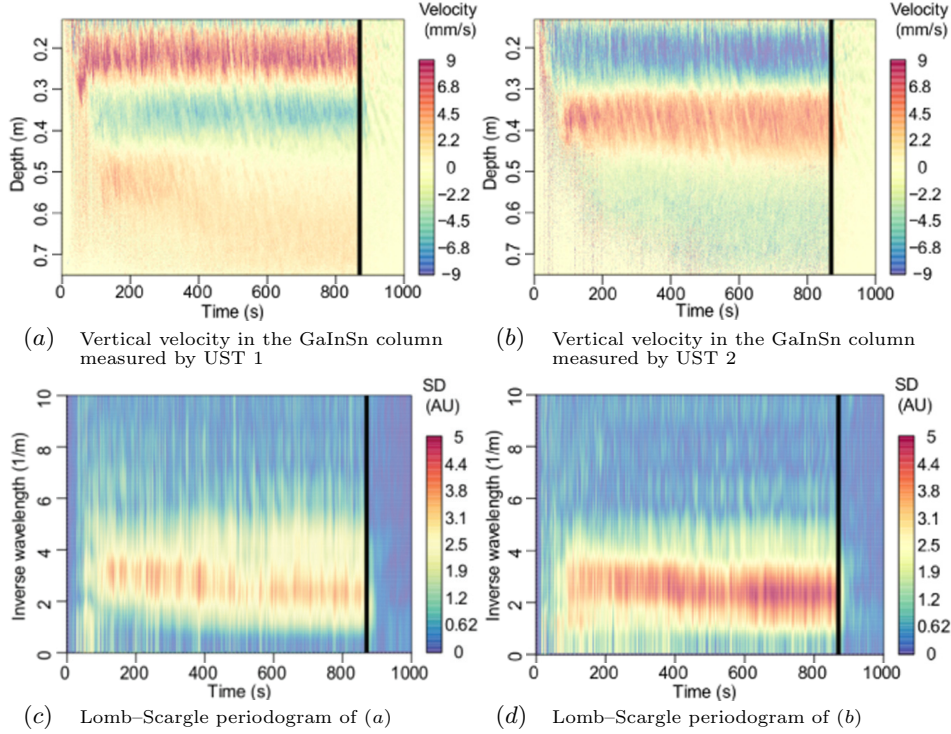


Fig. 5. Velocity profiles and periodograms at 2.00 kA. Current is cut off after 870 s (vertical black lines).

have been carried out and yielded velocity profiles at sub-critical currents that are qualitatively similar to those observed.

These results necessitate further analysis, such as the comparison of longitudinal growth rates of individual λ^{-1} bands with each other as well as with the growth rate derived from fluxgate magnetometer measurements and numerics. Furthermore, the effect of the magnetic field caused by the the conductors to and from the PSU must no longer be neglected and should be quantified.

A new top electrode, designed to accommodate four USTs arranged to illuminate four quadrants of the cylinder will provide more detail of the velocity field. Numerical investigations into the interplay of the various possible phenomena leading to the observed velocity profiles, i.e. electrode-driven electro-vortex flow, thermal convection and TI, are underway and a numerical study on the effects of electro-vortex flows and non-axisymmetric geometry of the conductors feeding the current to the experiment on the TI has been carried out [13].

3. Conclusion. It has been demonstrated that it is possible to perform meaningful UDV measurements inside media with currents of the order of 4 kA. Preliminary results show some agreement with previous magnetic field measurements, although it has not been shown yet that the growth rate of modes suspected of being caused by the TI are congruent with B_z measurement results. Four ultrasound sensors will be inserted into a new top electrode at 90° intervals in order to improve the azimuthal resolution of the vertical velocity measurements.

Acknowledgements. The work presented here received support from the Helmholtz Association of German Research Centres as part of the ‘‘Helmholtz-Initiative f#252;r mobile und station#228;re Energiespeichersysteme’’, in addition to the Helmholtz Alliance ‘‘Liquid Metal Technologies’’ (LIMTECH).

REFERENCES

- [1] K. WANG, *et al.* Lithium-antimony-lead liquid metal battery for grid-level energy storage. *Nature*, vol. 514 (2014), pp. 348–350.
- [2] H. KIM, *et al.* Liquid metal batteries: Past, present, and future. *Chemical Reviews*, vol. 113 (2013), no. 3, pp. 2075–2099.
- [3] F. STEFANI, T. WEIER, T. GUNDRUM, AND G. GERBETH. How to circumvent the size limitation of liquid metal batteries due to the Tayler instability. *Energy Conversion and Management*, vol. 52 (2011), no. 8, pp. 2982–2986.
- [4] N. WEBER, V. GALINDO, F. STEFANI, AND T. WEIER. Current-driven flow instabilities in large-scale liquid metal batteries, and how to tame them. *Journal of Power Sources*, vol. 265 (2014), pp. 166–173.
- [5] W.F. BERGERSON, *et al.* Onset and saturation of the kink instability in a current-carrying line-tied plasma. *Phys. Rev. Lett.*, vol. 96 (2006), art. no. 015004, pp. 1–4.
- [6] R. TAYLER. The adiabatic stability of stars containing magnetic fields—I: Toroidal Fields. *Monthly Notices of the Royal Astronomical Society*, vol. 161 (1973), no. 4, pp. 365–380.
- [7] H.C. SPRUIT. Dynamo action by differential rotation in a stably stratified stellar interior. *Astronomy & Astrophysics*, vol. 381 (2002), pp. 923–932.
- [8] G. RÜDIGER AND M. SCHULTZ. Tayler instability of toroidal magnetic fields in MHD Taylor-Couette flows. *Astronomische Nachrichten*, vol. 331 (2010), no. 1, pp. 121–129.
- [9] N. WEBER, *et al.* Numerical simulation of the Tayler instability in liquid metals. *New Journal of Physics*, vol. 15 (2013), art. no. 043034, pp. 1–19.
- [10] M. SEILMAYER, *et al.* Experimental evidence for a transient Tayler instability in a cylindrical liquid-metal column. *Phys. Rev. Lett.*, vol. 108 (2012), art. no. 244501, pp. 1–4.
- [11] M. SEILMAYER, F. STEFANI, AND T. GUNDRUM. Noise reduction of UDV measurements in liquid metal experiments with high magnetic fields. *Proceedings of the 9th International Symposium on Ultrasonic Doppler Methods for Fluid Mechanics and Fluid Engineering*, vol. 9 (2014), pp. 41–44.
- [12] J.D. SCARGLE. Studies in astronomical time series analysis. II - Statistical aspects of spectral analysis of unevenly spaced data. *The Astrophysical Journal*, vol. 263 (1982), pp. 835–853.
- [13] N. WEBER, *et al.* The influence of current collectors on Tayler instability and electro-vortex flows in liquid metal batteries. *Physics of Fluids*, vol. 27 (2015), no. 1, art. no. 014103.

Received 21.01.2015